Cross-sectional scanning tunneling microscopy and spectroscopy of passivated III–V heterostructures

S. Gwo,[a] A. R. Smith, K.-J. Chao, and C. K. Shih
Department of Physics, University of Texas, Austin, Texas 78712

K. Sadra[b] and B. G. Streetman
Microelectronics Research Center and Department of Electrical and Computer Engineering, University of Texas, Austin, Texas 78712

(Received 22 November 1993; accepted 11 April 1994)

Structural and electronic properties of $Al_{0.3}Ga_{0.7}As$/GaAs heterojunction and GaAs *pn* junction systems are investigated by cross-sectional scanning tunneling microscopy and spectroscopy (XSTM/S). The cross-sectional samples were prepared by passivating *ex situ* with a sulfide $[(NH_4)_2S]$ solution and were transferred into an ultra-high vacuum system for STM/S studies. It is found that passivated samples are advantageous for the measurements of scanning tunneling spectroscopy. The STM/S results and the experimental details are reported.

I. INTRODUCTION

Advances in semiconductor technology have made possible the ability to tailor the electronic structure of materials through stacking dissimilar materials into multilayered heterostructures. These heterostructures are the building blocks for many advanced electronic and optoelectronic devices. Since the desired properties of heterostructures originate from the formation of junctions, two fundamentally important topics are characterization of the junction morphology and revealing the electronic structure across the junction. Compared with the conventional approach using a combination of transmission electron microscope (TEM), x-ray diffraction (XRD), photoluminescence, $C-V$ measurement, or photoemission, cross-sectional scanning tunneling microscopy and spectroscopy (XSTM/S) can investigate the structural and electronic properties of heterostructures simultaneously on the atomic scale.[1–11]

Since STM is a surface-sensitive tool, it is very important to assure that the bulk electronic properties of heterostructures, such as band offsets, can be measured at the cross-sectional surface [usually, the (110) surface since most heterostructures are grown on the (001) substrate]. In the case of III–V compound semiconductor (110) surfaces, the intrinsic surface states lie outside of the fundamental band gap. As a result, the band-edge positions, as measured by tunneling spectroscopy, correspond to the band-edge positions within the bulk. This advantage makes compound semiconductor heterojunctions ideal candidates for XSTM/S studies. However, there is a severe tip-induced band bending effect in the tunneling spectroscopy of wide band-gap systems. This effect severely impedes the use of XSTM/S as a direct mapping tool across the heterojunctions.[2,3] We overcome this difficulty by passivating the cleaved cross-sectional surface with a sulfide solution[4,5] since the sulfur-induced surface states which pin the Fermi level also screen out the electric field.

II. EXPERIMENT

The III–V structures discussed in this work were grown on (001) substrates (n-type, 1×10^{18} cm^{-3}) using molecular-beam epitaxy (MBE). Epilayer doping concentrations in (AlGa)As/GaAs heterojunctions were: $n=2\times10^{18}$ cm^{-3} [Si] and $p=2\times10^{18}$ cm^{-3} [Be]. Epilayer doping concentrations for *pn* junctions were: $n=5\times10^{18}$ cm^{-3} [Si] and $p=1\times10^{19}$ cm^{-3} [Be]. The multilayered structures were grown at 600 °C for GaAs *pn* junctions and 620 °C for (AlGa)As/GaAs heterojunctions. Two Ga sources were employed to allow equal doping in GaAs and (AlGa)As layers. The growth of (AlGa)As/GaAs heterojunctions was performed without the interruption technique.

The passivation procedure used in this work is the following: first, samples are cleaved in air to expose the (110) faces and then dipped into a buffered $(NH_4)_2S$ solution (Fisher-Chemical, 21.1%) for 5–10 min. Following this soak, the $(NH_4)_2S$ solution is diluted thoroughly with de-ionized water before removing the samples. After this step, the samples are rinsed in the de-ionized water and blown dry with nitrogen gas. The conventional etching step used for (001) wafers (e.g., using 1:1:250 H_2SO_4:H_2O_2:H_2O etchant)[12] is skipped since we find a significant increase in surface roughness when the surface is treated with this etchant. No major difference results between cleaving inside the $(NH_4)_2S$ solution and cleaving in air. In our experiments, we also find that the purity of the de-ionized water plays an important role in determining the surface quality of the passivated samples. After the passivation process, the best of a group of cleaved and passivated samples are immediately transferred into the UHV chamber through a load-lock for STM experiments. The tungsten tunneling tips are cleaned *in situ* prior to the experiments by a field emission method on separate clean substrates.

Figure 1 is the schematic diagram of the epilayer edge-finding algorithm. After the sample is cleaved and transferred into the STM sample stage, the tip is first positioned near the

[a]Present address: Joint Research Center for Atom Technology, National Institute for Advanced Interdisciplinary Research, 1-1-4 Higasshi, Tsukuba, Ibaraki 305, Japan.
[b]Present address: Department of Electrical Engineering, University of Missouri, Columbia, MO 65211.

 0734-2101/94/12(4)/2005/4/$1.00

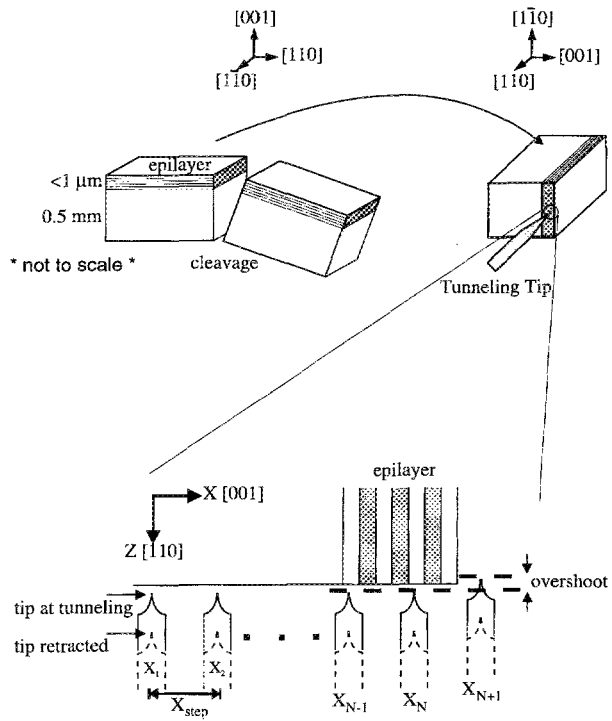

FIG. 1. Schematic diagram showing how the tip is positioned within the region of the epilayer.

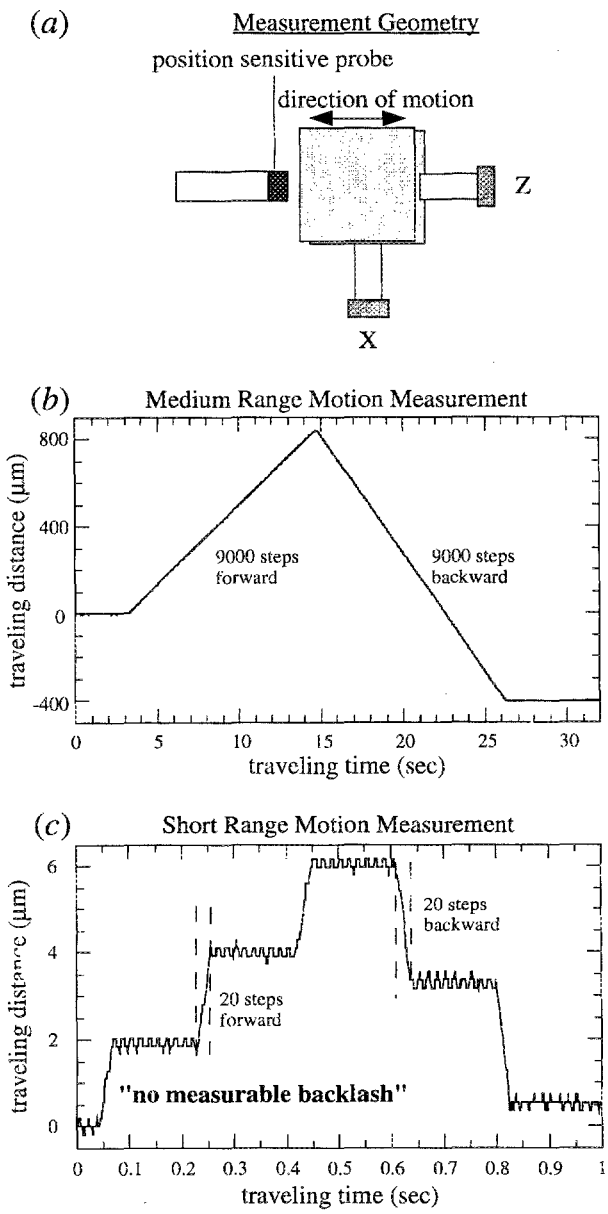

FIG. 2. Performance measuremetns of the sample walker: (a) measurement geometry; (b) medium-range motion measurement (9000 steps/time); and (c) short-range motion measurement (20 steps/time). Step size is about 200 Å.

edge of the epilayer region with the aid of an optical microscope. The tip is then brought into the tunneling regime by the auto-approach procedure. Subsequent iteration of recording the tip position, withdrawing the tip, stepping the sample laterally, and reapproaching the tip is used to detect the epi-edge of the (110) cleaved surface. This iteration process terminates when the z-piezo voltage drastically exceeds (shown as an overshoot) the previous voltage at which tunneling occurred. Stepping the sample laterally places the tip in the correct position to study the epilayer. The success of this method depends primarily upon two things. First, the sample must be extremely flat all the way up to the epi-edge. This is achieved in this work by choosing the best of a group of cleaved samples before transfer into the UHV-STM system for study. Second, a two-dimensional sample mover which is free of backlash and crosstalk is necessary. Shown in Fig. 2 is the performance measurement of the sample walker used for this work. If the epilayer thickness exceeds one micron, we often can directly bring the tip within the epilayer region by using the optical microscope without even applying the epilayer edge-finding algorithm.

III. RESULTS AND DISCUSSION

A. The advantages of pinned versus unpinned surfaces

In the past, it was considered that the major advantage of performing the XSTS band mapping technique on III–V heterostructure surfaces is their unpinned surface nature (as a result of intrinsic surface states residing outside of the fundamental band gap). However, it turned out later, by the studies of Salemink *et al.*,[2,3] that the tip-induced band bending imposes a serious constraint on precisely determining the band edge positions. The tip-induced band bending effect is particularly important for wide band-gap semiconductors such as GaAs (Ref. 13) and (AlGa)As. In the case of homogeneous GaAs, since the degree of tip-induced band bending depends on the doping level, this effect can be reduced by simply using heavily-doped samples. Unfortunately, for III–V heterojunction or pn junction samples, there are depleted regions right at the junctions of interest. Thus, the tip-induced band bending effect is inevitably a problem when studying unpinned III–V heterostructure surfaces. Ironically, the solution to this band-bending dilemma is to create a

strongly pinned surface since the extrinsic surface states which pin the Fermi level also screen out the electric field induced by the tunneling tip. The influence of the Fermi level pinning on the tip-induced band bending has been discussed in our earlier publication[5] as well as those of Feenstra and co-workers.[6,7] In our earlier publication, it was also discovered that the sulfide-passivation process described here produces a uniformly pinned cross-sectional surface, ideal for studies of heterojunctions.[5]

B. Passivated $Al_{0.3}Ga_{0.7}As$/GaAs heterojunctions

Tunneling spectroscopy results reported here are obtained on 64×64 pixel images where $I-V$ tunneling spectra were recorded at each pixel by interrupting the STM feedback momentarily. The majority of our data are analyzed by using a normalized conductivity $d(\ln|I|)/dV$ versus position method, where the conductivity is obtained by numerically differentiating the $I-V$ spectra. Normalized conductivity images can be directly used to represent the valence band or conduction band edges relative to the Fermi level. This can be understood when we consider that the tunneling current can be expressed as

$$I \propto \int_{eV_0}^{eV} \exp(-2\kappa S)\rho_s(E)dE,$$

where S is the tip-sample separation, κ is the decay constant, V is the bias voltage, V_0 is the band threshold, and $\rho_s(E)$ is the density of states of the sample at the energy E. We assume in this approximation that the density of tip states $\rho_t(E)$ is essentially constant. When $V \approx V_0$, we can use the parabolic band approximation for $\rho_s(E)$; therefore, $\rho_s(E) \propto (E-eV_0)^{1/2}$. To lowest order, the tunneling current I is proportional to $\exp(-2\kappa S)\ (V-V_0)^{3/2}$ (in general, κ is also bias voltage dependent; however, within a small bias window, we approximate it as a constant). In this approximation, the normalized conductivity, $d(\ln|I|)/dV=(dI/dV)/I \propto 1/(V-V_0)$, is a quantity independent of the tip-sample separation and diverges as $V \to V_0$. Thus, if the bias voltage is closer to the band edge, $d(\ln|I|)/dV$ will be larger. Indeed, as shown in Fig. 3(a), we can see that $d(\ln|I|)/dV$ at a constant sample bias is much larger in the (AlGa)As region, indicating the effect of the valence-band offset (VBO). Furthermore, the $1/(V-V_0)$ dependence of the $d(\ln|I|)/dV$ is also evident. In Fig. 3(b), we show an experimental $d(\ln|I|)/dV$ curve for GaAs along with a theoretical curve of $\alpha/(V-V_0)$ with $\alpha=1.75$ and $V_0=-0.6$ V. For most of our experimental data acquired on sulfide-passivated surfaces, we have found that $d(\ln|I|)/dV$ shows a $1/(V-V_0)$ dependence with α ranging from 1.5 to 2.4. The spatial dependence of the valence band maximum (VBM) can be estimated directly from the normalized conductivity plot since $V_0=V-\alpha[d(\ln|I|)/dV]^{-1}$. The approach of using the $d(\ln|I|)/dV$ plot offers an effective method for showing the spatial variation of electronic structure since it does not require any extra fitting parameters and since the exponential dependence of the tip-sample separation is removed.[5] In the following section, we will concentrate on the GaAs pn junction system.

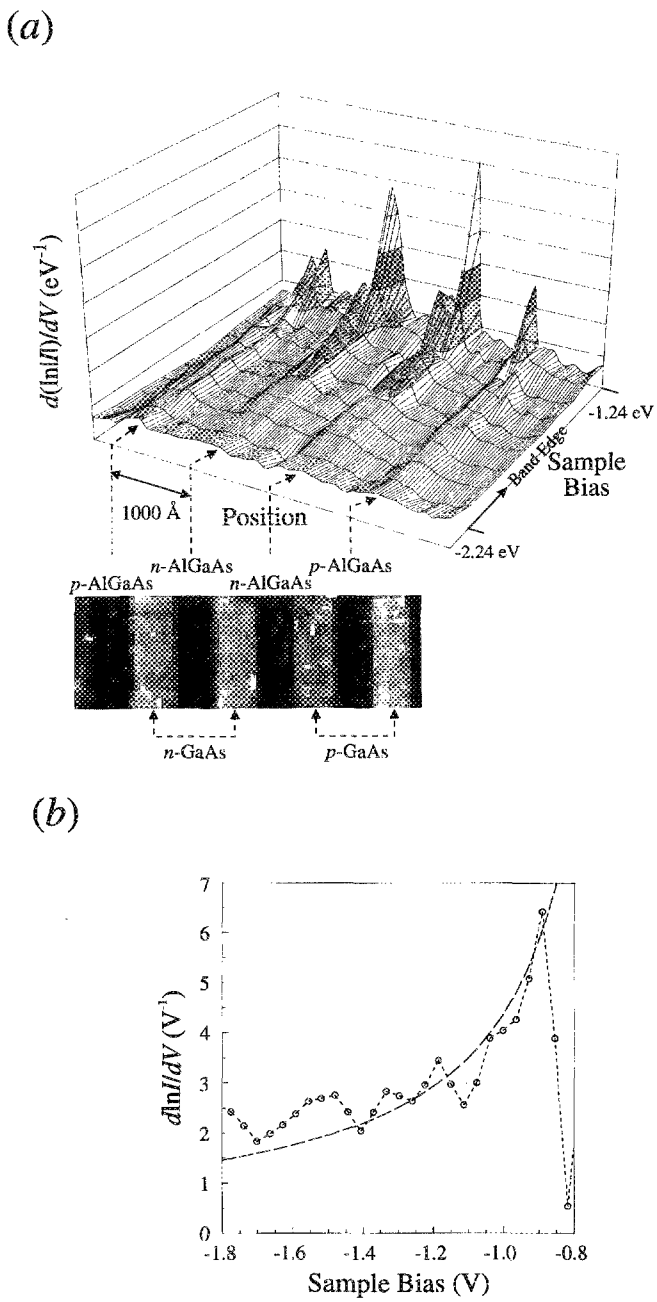

FIG. 3. (a) A plot of normalized conductivity vs position and bias over a scanning area of 4500 Å×1500 Å. The corresponding STM image acquired at a sample bias of −2.35 V and a tunneling current of 0.3 nA is displayed in the lower left corner. (b) An experimental $d(\ln|I|)/dV$ curve for GaAs along with a theoretical curve of $\alpha/(V-V_0)$ with $\alpha=1.75$ and $V_0=-0.6$ V.

C. Passivated GaAs *pn* junctions

Figure 4(a) shows a constant-current cross-sectional image of GaAs pn junction regions. The growth structure (also shown) consists of alternating n- and p-type regions having layer widths varying from 1000 to 2000 Å (with a total epilayer thickness of 10.6 μm). The p-type regions are doped 1×10^{19} cm^{-3} [Be] while the n-type regions are doped 5×10^{18} cm^{-3} [Si] which results in a depletion width of about 250 Å for an abrupt junction. Shown in Fig. 4(b) is the averaged topographic profile for the image. Three interesting

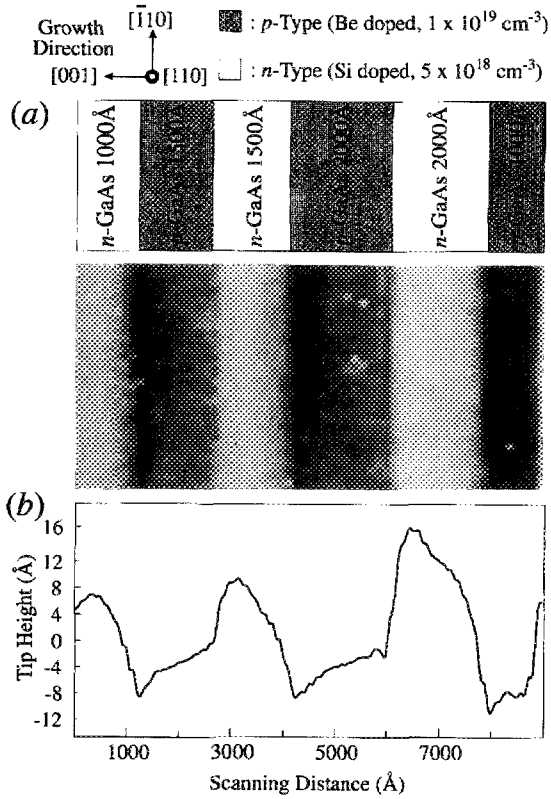

FIG. 4. A 9000 Å×600 Å (not to scale along the y-direction) STM image of GaAs *pn* junctions with layer widths of 1000, 1500, and 2000 Å each and a total epilayer thickness of 10.6 μm, acquired with a sample bias of −2.14 V and a tunneling current of 0.17 nA. Part (a) shows the image with the corresponding MBE growth structure while part (b) is the averaged topographic profile.

features in this figure need to be mentioned. First, the topographic height difference between *n*- and *p*-type regions appears to depend upon the layer width. In particular, wider regions show larger topographic height difference. Second, the magnitude of the height difference is quite large (ranging from 10 to 20 Å). This is in contrast to our results on UHV-cleaved samples with the same growth structure where the topographic height difference is about five times less. Third, neither *n*- nor *p*-type regions have a symmetrical topographic shape. The width of the transition region on the left-hand side of the bright *n*-type regions is very close to the depletion width for an abrupt junction, while on the right hand side the transition is much more gradual. Further investigation is currently under way to ascertain whether or not this asymmetry is related to the interdiffusion of dopants during the MBE growth process.

IV. SUMMARY

By studying sulfide passivated cross-sectional surfaces of (AlGa)As/GaAs superlattices and GaAs *pn* junctions, we have demonstrated that STM/S is capable of mapping out electronic structure across semiconductor junctions with nanometer resolution. Many important properties of semiconductor junctions not accessible by other techniques can now be investigated in detail by STM/S.[5]

In the (AlGa)As/GaAs system, we present both the topography and the simultaneously measured conductivity versus position and bias voltage plot. The lowest-order approximation of $d(\ln|I|)/dV=(dI/dV)/I\propto 1/(V-V_0)$ shows reasonable agreement with our data. For the GaAs *pn* junction system, much larger topographic contrast has been found between *n*- (brighter) and *p*-GaAs (darker) regions compared with the STM results performed on UHV-cleaved samples with the same growth structure. Interesting asymmetrical behavior has been found between the two transition regions within each layer. This behavior may be a result of the MBE growth process. Further study is under way.

ACKNOWLEDGMENTS

This work was supported by the Texas Advanced Research Program, the Joint Services Electronics Program (No. AFOSR F49620-92-C-0027), and the Science and Technology Center Program of NSF (No. CHE8920120). Financial support from the Trull Centennial Professorship in Physics Fellowship No. 1 is also acknowledged.

[1]O. Albrektsen, D. J. Arent, H. P. Meier, and H. W. M. Salemink, Appl. Phys. Lett. **57**, 31 (1990).
[2]H. W. M. Salemink, O. Albrektsen, and P. Koenraad, Phys. Rev. B **45**, 6946 (1992).
[3]H. W. M. Salemink, M. B. Johnson, U. Maier, P. Koenraad, and O. Albrektsen, *Semiconductor Interfaces at Subnanometer Scale*, NATO ASI Series E No. 243, edited by H. W. M. Salemink and M. D. Pashley (Kluwer, Dordrecht, 1993), p. 151.
[4]S. Gwo, K.-J. Chao, A. R. Smith, C. K. Shih, K. Sadra, and B. G. Streetman, J. Vac. Sci. Technol. B **11**, 1509 (1993).
[5]S. Gwo, K.-J. Chao, C. K. Shih, K. Sadra, and B. G. Streetman, Phys. Rev. Lett. **71**, 1883 (1993).
[6]R. M. Feenstra, A. Vaterlaus, E. T. Yu, P. D. Kirchner, C. L. Lin, J. M. Woodall, and G. D. Pettit, in Ref. 3, p. 127.
[7]A. Vaterlaus, R. M. Feenstra, P. D. Kirchner, J. M. Woodall, and G. D. Pettit, J. Vac. Sci. Technol. B **11**, 1502 (1993).
[8]S. Gwo, A. R. Smith, C. K. Shih, K. Sadra, and B. G. Streetman, Appl. Phys. Lett. **61**, 1104 (1992).
[9]R. M. Feenstra, E. T. Yu, J. M. Woodall, P. D. Kirchner, C. L. Lin, and G. D. Pettit, Appl. Phys. Lett. **61**, 795 (1992).
[10]T. Kato and F. Osaka, Jpn. J. Appl. Phys. **30**, L1586 (1991); T. Kato and F. Osaka, J. Appl. Phys. **72**, 5716 (1992).
[11]J. A. Dagata, W. Tseng, J. Bennett, J. Schneir, and H. H. Harary, Appl. Phys. Lett. **59**, 3288 (1991); Ultramicroscopy **42–44**, 1288 (1992).
[12]M. R. Melloch, M. S. Carpenter, T. E. Dungan, D. Li, and N. Otsuka, Appl. Phys. Lett. **56**, 1064 (1990).
[13]R. M. Feenstra and J. A. Stroscio, J. Vac. Sci. Technol. B **5**, 923 (1987).